SUNGKYUNKWAN UNIVERSITY
DEPARTMENT OF PHYSICS

Status Report

Donghun Jung

Quantum State Tomography and Coarse-Grained Positive Valued Measurement

This report summarizes my studies over two weeks until June 9 and is submitted on June 19, 2023.

Summary

Table of Contents

List of Figures

Chapter 1

Quantum State Tomography

Abstract

Quantum State Tomography (QST) is a method used to reconstruct a quantum state of a given system by performing a series of measurements in different measurement bases. The measurement process extracts information from the quantum state by measuring the distance between the hyperplane and the state vector. To reconstruct the full quantum state, there are two main methods for conducting QST: Maximum Likelihood Estimation(MLE) and Linear Regression Estimation(LRE).

1.1 Quantum State Tomography

Quantum State Tomography(QST) is the process of reconstructing a quantum state of a given system through a series of measurements in different (measurement) basis. Similar to its classical counterpart, Tomography, which reconstructs a three-dimensional image via a series of two-dimensional projections, QST aims to reconstruct a full or the most probable density matrix or wave function through multiple measurements. [1]

There are various statistical methods available to reconstruct the original quantum state, even from incomplete information. (3) However, in general, without a priori information, informationally complete or overcomplete mea-

[1]Due to the quantum nature, measuring a state of the given state perturbs its state. Therefore, QST must be conducted on a number of identical copied states.

surements are required, which is referred to as full quantum state tomography (FQST).

1.1.1 Informational approach to QST

From an informational approach, determining only one density matrix of a d-dimensional quantum system requires $2d^2$ variables. However, there are constraints on the density matrix. First, the density matrix must be Hermitian. Second, the density matrix must be positive semidefinite. Third, the trace of the density matrix must be 1. These constraints reduce the number of required variables to $d^2 - 1$, which means $d^2 - 1$ measurements are required to determine the state of a d-dimensional quantum system.

1.1.2 Mathematical approach to QST

From a mathematical perspective, the measurement process measures the distance between the hyperplane and the state vector. As discussed above, state vector is given by

$$\rho^i = \mathrm{tr}\left(\rho\Gamma^i\right) \tag{1.1}$$

where measurement basis is given by

$$\Omega^k = \theta_i^k \Gamma^i \tag{1.2}$$

Note that θ_i^k can be regarded as a normal vector of hyperplane of the measurement operator Ω^k in $\mathbf{R}^{d^2}$ space. Here, the result of the measurement can be written by

$$\begin{aligned} \left\langle \Omega^k \right\rangle &= \mathrm{tr}\left(\rho\Omega^k\right) && (1.3)\\ &= \theta_i^k \,\mathrm{tr}\left(\rho\Gamma^i\right) && (1.4)\\ &= \theta_i^k \rho^i && (1.5) \end{aligned}$$

That is, it is the inner product between the normal vector of hyperplane and the state vector. Although θ_i^k is not an unit vector, $\left\langle \Omega^k \right\rangle$ can be regarded as the distance between the hyperplane and the state vector. Therefore, QST is to determine the value of γ_i in the equation, given the normalization condition, $\gamma_0 = 1$. Since there are $d^2 - 1$ undetermined variables, $d^2 - 1$ measurements are required. Then, γ_i are determined uniquely since the space of density matrix is convex.

1.2 Methods for QST

The general idea reconstructing the given quantum state is to solve the following equation for Θ, which represents the elements in the vector form of a given quantum state ρ.(1)

$$X\Theta = P \tag{1.6}$$

where P is the measured frequency of the measurement operator Ω_i, and X is given by

$$X = \begin{pmatrix} \mathrm{Tr}(\Omega_1\Gamma^{00\cdots0}) & \mathrm{Tr}(\Omega_1\Gamma^{00\cdots1}) & \cdots & \mathrm{Tr}(\Omega_1\Gamma^{33\cdots3}) \\ \mathrm{Tr}(\Omega_2\Gamma^{00\cdots0}) & \mathrm{Tr}(\Omega_2\Gamma^{00\cdots1}) & \cdots & \vdots \\ \vdots & \vdots & \ddots & \vdots \\ \mathrm{Tr}(\Omega_M\Gamma^{00\cdots0}) & \cdots & \cdots & \mathrm{Tr}(\Omega_M\Gamma^{33\cdots3}) \end{pmatrix} \tag{1.7}$$

Then, it is expected to find the given density matrix:

$$\rho = \theta_{ij\cdots k}\Gamma^{ij\cdots k} \tag{1.8}$$

However, there are potential problems with this method. Firstly, the exact measurement is impossible due to the limited number of possible copies of the quantum state. Secondly, M may not be equal to $d^2 - 1$, the dimensionality of the quantum state. This can lead to an unsolvable equation, or even if solvable, may result in a density matrix that violates important properties such as positive semidefiniteness and normalization. To overcome these problems, two alternative numerical methods exist for obtaining a physically valid density matrix.

1.2.1 Maximum Likelihood Estimation

Maximum Likelihood Estimation(MLE) method finds the density matrix that is most likely to have produced the observed measurement outcomes. Any positive semidefinite matrix $\mathcal{G}$ that satisfies $\langle\psi|\,\mathcal{G}\,|\psi\rangle \geq 0$ can be expressed as $\mathcal{G} = \hat{T}^\dagger\hat{T}$, where $\hat{T}$ is a tridiagonal matrix chosen for convenience.(2) For a two-qubit system, $\hat{T}$ can be written as:

$$\hat{T} = \begin{pmatrix} t_1 & 0 & 0 & 0 \\ t_5 + it_6 & t_2 & 0 & 0 \\ t_{11} + it_{12} & t_7 + it_8 & t_3 & 0 \\ t_{15} + it_{16} & t_{13} + it_{14} & t_9 + it_{10} & t_4 \end{pmatrix} \tag{1.9}$$

Furthermore, any manifestly physical density matrix can be written as:

$$\rho = \frac{\hat{T}^\dagger \hat{T}}{\mathrm{Tr}(\hat{T}^\dagger \hat{T})} \tag{1.10}$$

whether the density matrix is pure state or not. It is important to note that $\mathcal{G}$ must be Hermitian.

Let me assume that the noise on the coincidence measurements has a Gaussian distribution. Then, the probability of obtaining a measurement result n_{real} given a theoretical expectation value n_{exp} is given by:

$$p = \mathcal{N}_{\mathrm{norm}} \prod_i \exp\left[-\frac{(n^i_{\mathrm{real}} - n_{\mathrm{exp}})^2}{2\sigma_i^2}\right] \tag{1.11}$$

where the expectation value for ith measurement is given by $n^i_{\mathrm{ext}} = \mathrm{Tr}(\rho\Omega^i)$. Here, the standard deviation for the ith measurement can be approximated to $\sqrt{n^i_{\mathrm{exp}}}$. Then, the likelihood function is rewritten by:

$$p = \mathcal{N}_{\mathrm{norm}} \prod_i \exp\left[-\frac{(n^i_{\mathrm{real}} - N\,\mathrm{Tr}\,\rho\Omega^i)^2}{2N\,\mathrm{Tr}\,\rho\Omega^i}\right] \tag{1.12}$$

where N is the total number of observation for the measurement operator Ω^i. Here it is assumed that N is equal for every measurement. Finally, the parameters t are chosen to maximize the likelihood function or, equivalently, minimize the following function:

$$\mathcal{L} = \sum_i \frac{(n^i_{\mathrm{real}} - N\,\mathrm{Tr}\,\rho\Omega^i)^2}{2N\,\mathrm{Tr}\,\rho\Omega^i} \tag{1.13}$$

$$= \sum_i \frac{(p^i_{\mathrm{real}} - \mathrm{Tr}\,\rho\Omega^i)^2}{2\,\mathrm{Tr}\,\rho\Omega^i} \tag{1.14}$$

where $p^i = \frac{n^i_{real}}{N}$.

MLE method can be implemented with scipy.minimize or cvxopt in python.

1.2.2 Linear Regression

As seen, FQST requires a minimum of $d^2 - 1$ measurement operators, leading to a large number of measurements and a high computational time

complexity for data processing due to the curse of dimensionality. On the other hand, the MLE method requires d^2 variables, but a well-known method exists to solve the (possibly) unsolvable equation 1.6. This method, known as least-squares estimation, gives a direct estimate of Θ_{LS} as:

$$\Theta_{\mathrm{LS}} = (X^T X)^{-1} X^T P \tag{1.15}$$

Then, the density matrix can be directly reconstructed as:

$$\mu_{\mathrm{LS}} = \theta^{\mathrm{LS}}_{ij\cdots k} \Gamma^{ij\cdots k} \tag{1.16}$$

However, the recovered density matrix μ_{LS} may not satisfy the physical properties of a density matrix. To resolve this issue, a fast algorithm introduced in this letter (5) can be used. This algorithm, like the MLE method, uses the likelihood function given in equation 1.12 and finds the nearest physical density matrix under the 2-norm.

Chapter 2

Measurement basis

2.1 Introduction

In Full Quantum State Tomography (FQST), a minimum of $d^2 - 1$ measurement operators is required. While single-shot measurements, which can identify the state directly, are possible in systems such as optical or superconductor systems, our setup using the NV center in a diamond as a qubit does not allow for single-shot measurements. Instead, we rely on the number of photons emitted from the NV system, but the origin of each photon remains unknown. Thus, the measurement does not provide information about a specific state but rather includes mixed information.

For two-qubit system, the following measurement operators Ω^i are implemented.

$$\Omega^i = U_i^\dagger \frac{1}{2} \left(|0\rangle\langle 0| \otimes I_2 + I_2 \otimes |0\rangle\langle 0| \right) U_i \tag{2.1}$$

where U_i represents an arbitrary unitary operator implementable in a quantum circuit. These measurement operators possess three eigenstates, resulting in extracted information that does not originate from a particular state. Therefore, we refer to this series of measurements as Coarse-Grained measurement.

2.2 Measurement Process

The measurement process for a given PVM operator yields the number of photons emitted from the qubit. The expected number of photons, denoted

as n^i, can be calculated using the formula:

$$n^i = N \left\langle \Omega^i \right\rangle = N \operatorname{Tr} \hat{\rho} \Omega^i \tag{2.2}$$

where N represents the maximum number of detected photons. [1] The measurement process is noting but determining the distance between the hyperplane representing the PVM operator and the vector representing the density matrix in a d^2-dimensional real space.

2.2.1 Mapping a density matrix and a PVM operator into d^2-dimensional space

Let ψ^i represent the state vector corresponding to the given density matrix. Using a carefully chosen basis Γ^i, each component of the state vector can be expressed as:

$$\psi^i = \operatorname{Tr} \hat{\rho} \Gamma^i. \tag{2.3}$$

One of the basis vectors can be chosen as the identity operator, $\Gamma^0 = I$, and the normalization condition for the density matrix gives $\operatorname{Tr} \rho \Gamma^0 = 1$. In the case of a single qubit system, the $|0\rangle$ state can be represented by the density matrix:

$$\hat{\rho} = |0\rangle\langle 0| = \begin{pmatrix} 1 & 0 \\ 0 & 0 \end{pmatrix} \tag{2.4}$$

in a density matrix form.[2] Then, the state vector is given by

$$\psi = (1, 0, 0, 1) \tag{2.5}$$

where only three terms are necessary to represent the density matrix. This state vector can be mapped onto the Bloch sphere as shown in the figure 2.1, with a trivial constraint that it lies within the sphere satisfying the condition:

$$\langle \sigma_x \rangle^2 + \langle \sigma_y \rangle^2 + \langle \sigma_z \rangle^2 \leq 1. \tag{2.6}$$

Similarly, in a two-qubit system with four dimensions, the basis vectors can be chosen as $\Gamma^{ij} = \sigma^i \otimes \sigma^j$, where $i, j = 0, 1, 2, 3$ and σ^i represents the

[1] The number of detected photons fluctuates between n_0 and n_1 due to Rabi precession. Here, $N = n_1 - n_0$.

[2] The density matrix form is more general than wave function form since there exist a mixed state that can not be represented by wave function form.

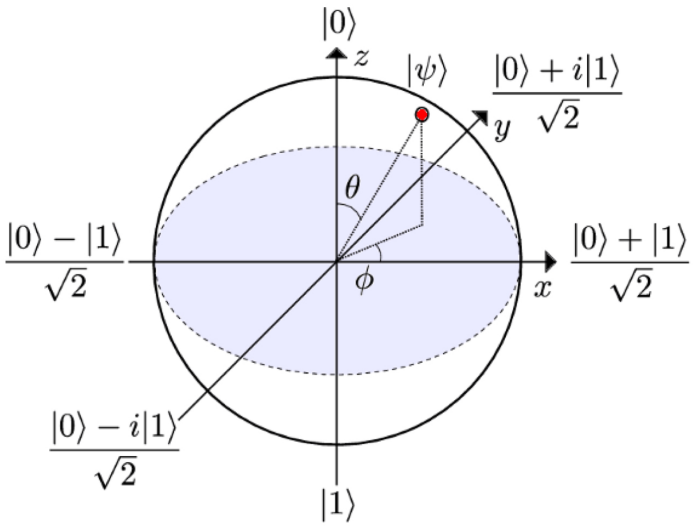

Figure 2.1: Bloch Sphere

Pauli matrices. Additionally, $\operatorname{Tr}\rho\Gamma^{00} = 1$. The state vector in this case is given by:

$$\vec{\psi} = \left(1, \operatorname{Tr}\hat{\rho}\Gamma^{01}, \operatorname{Tr}\hat{\rho}\Gamma^{02}, \cdots, \operatorname{Tr}\hat{\rho}\Gamma^{33}\right), \tag{2.7}$$

On the other hand, any PVM operator can be represented as a linear combination of the same basis:

$$\Omega^k = \sum_{i=0}^{d} \theta_i^k \Gamma^i \tag{2.8}$$

For example, consider the PVM operator:

$$\Omega^1 = \begin{pmatrix} \frac{1}{2} & \frac{1-i}{4} \\ \frac{1+i}{4} & \frac{1}{2} \end{pmatrix} = \frac{1}{2}I + \frac{1}{4}\sigma^1 + \frac{1}{4}\sigma^2 \tag{2.9}$$

which leads to the coefficients:

$$\vec{\theta} = \left(\frac{1}{2}, \frac{1}{4}, \frac{1}{4}, 0\right) \tag{2.10}$$

Therefore, the result of the measurement is given by

$$\left\langle \Omega^k \right\rangle = \operatorname{Tr} \hat{\rho}\Omega^i \tag{2.11}$$

$$= \sum_i \theta_i^k \operatorname{Tr} \hat{\rho}\Gamma^i \tag{2.12}$$

$$= \sum_i \theta_i^k \psi_i \tag{2.13}$$

$$= \vec{\theta_i^k} \cdot \vec{\psi} \tag{2.14}$$

Although not necessary, normalizing this result by $\left|\vec{\theta_i^k}\right|$ gives the distance between the hyperplane, defined by the normal vector θ_i^k, and the state vector $\vec{\psi}$. It is important to note that this normalization is not essential, as the length of the normal vector remains the same for the given PVM set, since the unitary operator acts as a rotational operator.

2.3 Optimal QST

In order to enable FQST, it is crucial to ensure that the rank of the PVM set is 15, as discussed earlier as the minimum number of measurements required. However, optimizing the QST process presents a separate challenge. Each measurement extracts three pieces of information[3] simultaneously from the quantum system, and conducting a uniform measurement operation on all elements in the PVM set can introduce non-uniformity in terms of the Pauli basis representation. To achieve optimal QST, it is desirable to have independent and less correlated measurement bases. This parallels classical tomography, where a three-dimensional image is reconstructed from a series of two-dimensional projections. The more independent or less correlated the measurement bases are, the more optimal the QST is expected to be.

To assess the quality of PVM sets and quantify their effectiveness, various metrics can be employed. These metrics serve as indicators to evaluate the performance and optimality of the PVM sets in the context of QST. By employing these metrics, researchers can assess how well the PVM sets capture the relevant information from the quantum system under investigation. These metrics provide a quantitative measure of the quality and reliability of the obtained quantum state reconstruction.

2.3.1 Gram matrix

The Gram matrix Π associated with the PVM set is a Hermitian and symmetric matrix, where each entry represents the Hilbert-Schmidt product of the corresponding PVM operators:

$$\Pi_{ij} = \mathrm{Tr}\,\Omega^i\Omega^j \tag{2.15}$$

The eigenvalues of the Gram matrix can be obtained through the Fourier transform of its rows, and the number of non-zero eigenvalues determines the rank of the PVM set.(4)

2.3.2 Hilbert-Schmidt norm of Gram matrix

The correlation between two PVM operators Ω^m and Ω^n can be quantified by the inner product of their respective normal vectors, $\sum_i \theta_i^m \theta_i^n$. If the

[3]It is because the rank of our PVM operator is 3.

normal vectors are orthogonal, it indicates that the two PVM operators are independent. Consequently, the correlation between the PVM operators can be evaluated using $(\sum_i \theta_i^m \theta_i^n)^2$. For a given PVM set, the overall correlation N among its elements is given by:

$$N = \sum_{m,n=0,1,\cdots} \left(\sum_i \theta_i^m \theta_i^n \right)^2 \tag{2.16}$$

$$= \frac{1}{2} \sum_{m,n=0,1,\cdots,(m\neq n)} (\mathrm{Tr}\, \Omega^m \Omega^n)^2 \tag{2.17}$$

$$= \frac{1}{2} \sum_{m,n=0,1,\cdots,(m\neq n)} (\Pi^{mn})^2 \tag{2.18}$$

$$= \frac{1}{2} \left(||\Pi|| - \sum_{m=0,1,\cdots} (\mathrm{Tr}\, \Omega^m \Omega^m)^2 \right) \tag{2.19}$$

In the above expression, the second term is constant. Therefore, the Hilbert-Schmidt norm of the Gram matrix serves as a metric to assess the correlation among the PVM set elements.

2.3.3 Neumann Entropy of Gram matrix

Given the Gram matrix, its eigenvalues are denoted as $e_0, e_1, \cdots$. After normalizing the eigenvalues by dividing each by the sum of all eigenvalues, denoted as $\sum_j e_j$, the von Neumann entropy S of the PVM set can be defined as(2)(6):

$$S = -\sum_i e_i' \ln e_i' \tag{2.20}$$

This can also be expressed as:

$$S = -\,\mathrm{Tr}\, \Pi' \ln \Pi' \tag{2.21}$$

where Π' is a normalized Gram matrix such that $\mathrm{Tr}\, \Pi = d$. The rank of the PVM set corresponds to the number of non-zero eigenvalues, and the saturation condition that maximizes the entropy ensures a full rank PVM set. This saturation condition is met when $e_i = e_j$ for all i and j. Each eigenvalue represents the amount of information obtained with respect to

a particular basis.[4] Moreover, the number of photons n_i' associated with a specific basis Γ_i is roughly proportional to Ne_i'. Additionally, Poisson noise is inversely proportional to $\frac{1}{\sqrt{n_i'}}$. By minimizing the sum of errors across all bases, it can be deduced that the errors should have the same scale for all bases, aligning with the condition of maximum entropy. Therefore, von Neumann entropy serves as a suitable metric since maximizing entropy is expected to guarantee stable QST with minimal error and a full rank PVM set, as dictated by the saturation condition.

[4]The reason have not been clearly understood yet.

2.4 Ideal QST

2.4.1 SIC POVM

In order to achieve an ideal quantum state tomography (QST), it is crucial to utilize an unbiased measurement scheme. One such ideal case is represented by a symmetric-informationally-complete POVM (SIC POVM). A measurement with a SIC POVM is referred to as informationally complete, as it allows for the complete determination of the target quantum state when the measurement is error-less.

The symmetry of the SIC POVM ensures that the Hilbert-Schmidt inner product between all the elements in the set is equal. This property enables the extraction of information from the quantum system in a uniform manner. Additionally, for maximal efficiency in determining the state, each measurement operator or POVM element should have a rank of 1. 2.2b This means that the operators are positive multiples of projectors onto pure states, allowing for the direct determination of the state represented by the given density matrix.

The SIC POVM possesses the following desirable properties:

1. Each POVM element has a rank of 1.
2. The number of elements in the POVM set is d^2, where d represents the dimension of the quantum state.
3. The Hilbert-Schmidt inner product between the POVM elements is given by $\frac{\mathrm{Tr}\,\Omega^i\Omega^j}{d^2} = \frac{d\delta^{ij}+1}{d+1}$.

However, it is important to note that the existence of SIC-POVM is currently only known for a few limited dimensions. For example, in the case of a two-qubit system, the von Neumann entropy is approximately 2.59. Analytical solutions for SIC POVM in higher dimensions are still under investigation. In the following paper (7), an analytical solution for the two-qubit system with a dimension of 4 is proposed.

Let us define the following variables:

$$r_0 = \frac{1-\frac{1}{\sqrt{5}}}{2\sqrt{2-\sqrt{2}}} \qquad r_1 = (\sqrt{2}-1)r_0 \qquad r_\pm = \frac{1}{2}\sqrt{1+\frac{1}{\sqrt{5}} \pm \sqrt{\frac{1+\sqrt{5}}{5}}}$$

$$a = \arccos \frac{2}{\sqrt{5+\sqrt{5}}} \qquad\qquad b = \arcsin \frac{2}{\sqrt{5}}$$

$$\Theta = \Bigg\{ \Bigg((-1)^m \left(\frac{a}{2} + \frac{b}{4} \right) + \pi \frac{m+2n+7j+1}{4}, \\ \frac{\pi(2k+1)}{2}, (-1)^m \left(-\frac{a}{2} + \frac{b}{4} \right) + \pi \frac{m+2n+3j+4k+1}{4} \Bigg) \\ \Bigg| k, j, m = 0, 1 \text{ and } n = 0, \cdots, 3 \Bigg\}$$

With these variables, the SIC POVM set for the two-qubit system can be expressed as:

$$\Bigg\{ \Omega^i = |\phi_i\rangle\langle\phi_i| \Bigg| |\phi\rangle = \begin{pmatrix} r_0 \\ r_+ e^{i\theta_+} \\ r_1 e^{i\theta_1} \\ r_- e^{i\theta_-} \end{pmatrix}, \text{ vectors generated by cycling of elements} \\ , \cdots, \begin{pmatrix} r_0 \\ r_- e^{i\theta_-} \\ r_1 e^{i\theta_1} \\ r_+ e^{i\theta_+} \end{pmatrix} \text{and } (\theta_1, \theta_\pm) \in \Theta \Bigg\}$$

Please note that the given equations and construction of the SIC POVM set for a two-qubit system with a dimension of 4 are provided as an example to illustrate the concept. Analytical solutions for SIC POVM in other dimensions are currently being explored.

Remark 1: Limitations of Implementing SIC POVM In our set-up, the implementation of SIC POVM is not feasible. This is due to the constraints imposed by our basic measurement, as described in the equation 2.1, which has a rank of 3. SIC POVM, which requires a higher number of elements, cannot be realized within these limitations.

Remark 2: Informational Completeness and Measurement Constraints If it were possible to perform measurements using SIC POVM, the outcomes would need to be distinguishable in order for the observer to identify the measured state. The informational completeness condition of

SIC POVM ensures that all relevant information about the quantum state can be obtained from a single measurement. However, in our specific set-up with only one detector, we can only distinguish between two states: the photon-emitted state and the non-photon-emitted state. As a result, each measurement process involves two POVMs, Ω^i and $I - \Omega^i$, to capture the information without loss. In order to perform QST, 16 measurement processes are required, explaining why the trace of our PVM is 2 compared to the $\frac{1}{4}$ trace of SIC POVM or GSIC POVM. Normalization is necessary before calculating the von Neumann entropy due to these difference.

2.4.2 The General Symmetric Informationally Complete POVM (GSIC POVM)

An alternative to rank-1 SIC POVMs is the concept of a general symmetric informationally complete POVM (GSIC POVM). Unlike SIC POVMs, GSIC POVMs are not necessarily of rank 1. The existence of GSIC POVMs has been shown for all dimensions, making them a useful criterion to assess the performance of our POVM set relative to an ideal measurement.

A POVM set is considered a GSIC POVM if it satisfies the following trace conditions for all i and j, where the values of a and b depend only on the dimension d:

$$\operatorname{Tr} G_i^2 = a \tag{2.22}$$

$$\operatorname{Tr} G_i G_j = b \tag{2.23}$$

These trace conditions can be represented by a Gram matrix Π:

$$\begin{pmatrix} a & b & \cdots & b \\ b & a & \cdots & \vdots \\ \vdots & \vdots & \ddots & \vdots \\ b & b & \cdots & a \end{pmatrix} \tag{2.24}$$

GSIC POVMs can be constructed using a complete orthogonal basis (COB) set A_i. The COB set satisfies two conditions:

1. Suborthogonality $\operatorname{Tr} A_i A_j = \frac{1}{d}\delta_{ij}$
2. Completeness $\sum_i A_i = \mathbb{I}$

The GSIC POVM is then given by:

$$G_i = \lambda A_i + (1-\lambda)\frac{\mathbb{I}}{d^2} \tag{2.25}$$

where $0 < \lambda \leq \frac{1}{1+d^2\tau}$ and $\tau = \max\{|m_i||m_i : \text{the minimum eigenvalue of} A_i\}$ The constructed GSIC POVM set satisfies the conditions mentioned earlier. Firstly, the completeness of the GSIC POVM set is automatically achieved by the completeness of the COB. Secondly, the positivity of the GSIC POVM is guaranteed if $\lambda\omega + (1-\lambda)\frac{1}{d^2} \geq 0$, where ω is the minimum eigenvalue of the COB set. Finally, the symmetry property is ensured by the trace conditions, resulting in a symmetric Gram matrix.:

$$\begin{aligned}
\operatorname{Tr} G^i G^j &= \operatorname{Tr}\left(\lambda A^i + (1-\lambda)\frac{I}{d^2}\right)\left(\lambda A^j + (1-\lambda)\frac{I}{d^2}\right) \\
&= \lambda^2 \operatorname{Tr} A^i A^j + \frac{(1-\lambda)\lambda}{d^2}\left(\operatorname{Tr} A^i + \operatorname{Tr} A^j\right) + \frac{(1-\lambda)^2}{d^4}\operatorname{Tr} I \\
&= \lambda^2 \frac{\delta^{ij}}{d} + \frac{1-\lambda}{d^3}
\end{aligned}$$

The main challenge in constructing a GSIC POVM lies in generating the COB. Given an orthonormal basis Γ^i that satisfies $\operatorname{Tr}\Gamma^i\Gamma^j = 0$ and an orthogonal $d^2 \times d^2$ real matrix O with $O_{0i} = \frac{1}{d\sqrt{d}}$, the COB can be constructed as:

$$A_i = \frac{1}{\sqrt{d}} \sum_{j=0}^{d^2-1} O_{ij}\Gamma^j \tag{2.26}$$

$\{\Gamma^i\}$ can easily generated, for example, the generator of $SU(d)$ but it may be challenging for constructing the orthogonal $d^2 \times d^2$ real matrix O. While an analytical solution for the COB is yet to be found (for me), a numerical solution is available for a GSIC POVM that may be implementable in our POVM set. This numerical solution provides an upper bound on the performance, with an entropy of approximately 1.539.

2.4.3 Conventional QST

In conventional quantum state tomography (QST) for two-qubit systems, the most general projective measurement (PVM) set can be defined. This PVM set, denoted as $\{\Omega^{ij}\}_{i,j=0,1,2,3}$, consists of four elements given by:

$$\Omega^{ij} = |i\rangle\langle i| \otimes |j\rangle\langle j| \tag{2.27}$$

where the basis states are represented as follows:

$$|0\rangle = \begin{pmatrix} 1 \\ 0 \end{pmatrix} \tag{2.28}$$

$$|1\rangle = \begin{pmatrix} 0 \\ 1 \end{pmatrix} \tag{2.29}$$

$$|2\rangle = |+\rangle = \frac{1}{\sqrt{2}}(|0\rangle + |1\rangle) \tag{2.30}$$

$$|3\rangle = |i\rangle = \frac{1}{\sqrt{2}}(|0\rangle + i\,|1\rangle) \tag{2.31}$$

It is important to note that while these PVM operators are not implementable in our specific setup, they can be implemented in optical or superconducting setups. The von Neumann entropy associated with the conventional PVM set is approximately 2.172. Conventional QST aims to reconstruct the quantum state of a two-qubit system using this PVM set. It provides a general approach for characterizing the quantum state and understanding its properties relativly easily.

2.5 PVM Set Construction Strategy

2.5.1 Strategy to Construct the PVM Set for a 2-qubit System

To construct the PVM set for a 2-qubit system using the given basic measurement operators 2.1, we can utilize unitary operators implemented with Pauli rotation gates and CZ gate. However, it is important to note that using the CZ gate can introduce a trade-off that may reduce gate fidelity.

Considering this trade-off, we aim to minimize the number of CZ gates while ensuring the PVM set spans the full $\mathcal{L}(\mathcal{H})$, where $\mathcal{H}$ is the d-dimensional Hilbert space. Without using the CZ gate, we can achieve a PVM set with a rank of 7. By including one CZ gate, we can construct a PVM set that spans $\mathcal{L}(\mathcal{H})$ and consists of 9 PVM operators.

These PVM operators can be implemented using a specific quantum circuit. The exact circuit diagrams are shown in the figure 2.2.

We can then choose 100 parameters that maximize the von Neumann entropy. For this case, the maximum von Neumann entropy achieved was

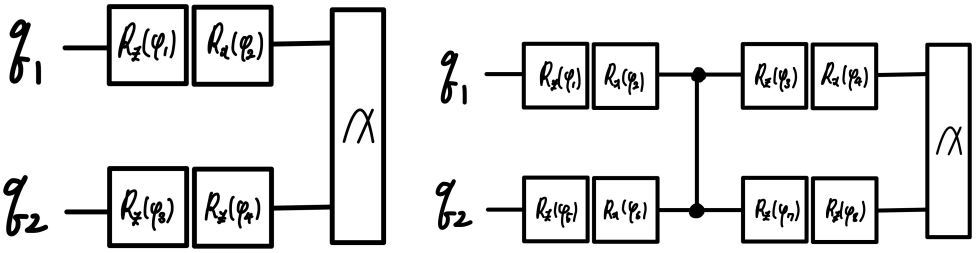

(a) None CZ Gate PVM operator (b) One CZ Gate PVM operator

Figure 2.2: Implementation of PVM operator on a quantum circuit

1.516. If we were allowed to use the CZ gate for all PVM operators, the entropy of 1.539 could be achieved.

2.5.2 Strategy to Construct the PVM Set for 3 and 4-qubit Systems

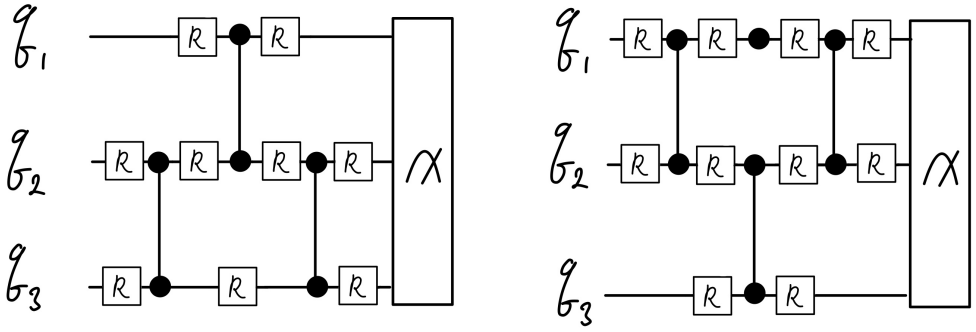

Figure 2.3: Implementation of PVM operator on a quantum circuit with 3 CZ gate for three-qubit system

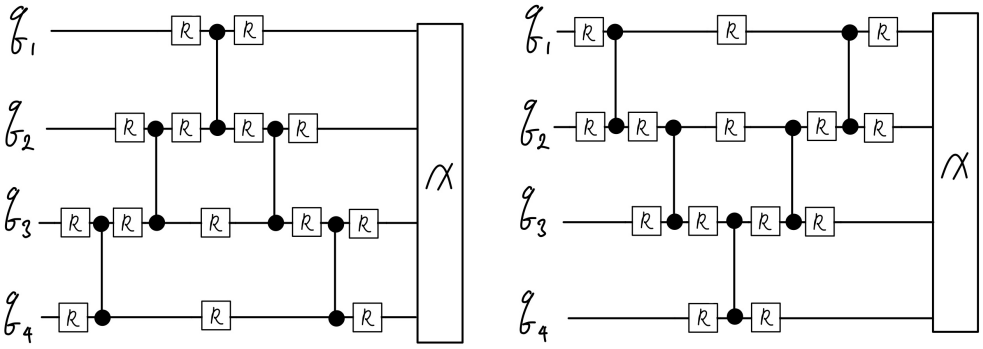

Figure 2.4: Implementation of PVM operator on a quantum circuit with 5 CZ gate for four-qubit system

A similar strategy can be applied to construct the PVM set for 3 and 4-qubit systems. Initially, we check the maximum rank of the Gram matrix without using the CZ gate. In order to fully span $\mathcal{L}(\mathcal{H})$, we gradually increase the number of CZ gates while checking the maximum rank of the Gram matrix.

In this process, the parameter θ^k mentioned in Equation 2.8 can be helpful. The number of non-zero values of θ represents the maximum number of dimensions that can be spanned by the given PVM operator.

Note that R represents a rotational operator that contains two parameters:

$$R^i = R_z(\phi^i)R_x(\theta^i) \tag{2.32}$$

Using this strategy, we find that $\mathcal{L}(\mathcal{H})$ for a three-qubit system can be fully spanned by using 3 CZ gates. The specific quantum circuit diagrams are shown in the figure 2.3.

For a four-qubit system, $\mathcal{L}(\mathcal{H})$ can be fully spanned by using 5 CZ gates as shown in the figure 2.4. It is important to note that since the quantum circuit is symmetric, the resulting space is also symmetric. Therefore, although the PVM operators using 5 CZ gates may not individually span $\mathcal{L}(\mathcal{H})$, by arranging the CZ gates differently, $\mathcal{L}(\mathcal{H})$ can be spanned effectively.

Chapter 3

QST Simulation result for two-qubit system

3.1 QST simulation process

3.1.1 Preparing target state $\rho^{\mathbf{target}}$

The target state preparation involved 10 randomly generated states denoted as $\{\rho_i^{\text{target}}\}_{i,j=1,\cdots,10}$. Although the number of target states was small, a significant number of QST simulations were performed. Unfortunately, some of the data was lost due to my mistake. To ensure that the chosen PVM operator set remains independent of specific target states, a uniform distribution was employed. This approach maintained the symmetry of the gram matrix for the prepared states. Initially, the harr random generation technique was intended for generating the target states. However, it should be noted that this method is only applicable for pure states in the `qutip` package. Surprisingly, it was previously believed that the distinction between pure and mixed states had no significant impact on the QST results during the QST simulation. However, a recent realization has highlighted the influence of target state purity on measurement errors and the QST process. Although further simulations may be required, this issue does not significantly affect the main findings of the study. The target states were randomly generated using the `qutip.rand_dm` function. For detailed information about the target states, refer to Appendix 6.1.

3.1.2 Preparing PVM operator set

To evaluate the effectiveness of QST with the PVM operator set designed according to our strategy, the PVM set provided in Appendix 6.26.3 was utilized. The entropy of this set, which is considered the best result based on our strategy, was measured to be 1.516. In our specific experimental setup, the entropy reached 1.539, which was regarded as the best outcome.

3.1.3 Measurement Process

In the actual experiment, a photodetector is used to count the number of photons emitted from the NV center qubit. The measurement frequency $f_i = \frac{n_i}{N}$ represents the raw data obtained from the measurement process. Here, N refers to the total number of shots, which corresponds to the total number of trials of measurement[1]. For convenience, the term "total number of shots" will be used to refer to N. The expectation value of n_i is given by $\mathrm{Tr}\,\rho^{\mathrm{target}}\Omega^i$, and the resulting error or noise in the measurement process follows a Poisson distribution. In the simulation, N is set to be 50,000, and an equal number of shots are taken for all measurements. To assess the tolerance of the PVM operator set against Poisson error, the simulation generates n_i with Poisson error, and 100 measurements are performed per target state. The `numpy.random.poisson` function is used to generate random Poisson error in this context.

[1] See 1

3.2 QST result

3.2.1 QST performance

The results of the QST simulation are presented as box plots in Figure 3.1. While there are some outliers in both PVM sets, they are considered tolerable since the average QST result exceeds 0.99. If the best PVM set could be implemented consistently, even better QST results could be achieved, as seen in the QST simulation for $S = 1.539$ states.

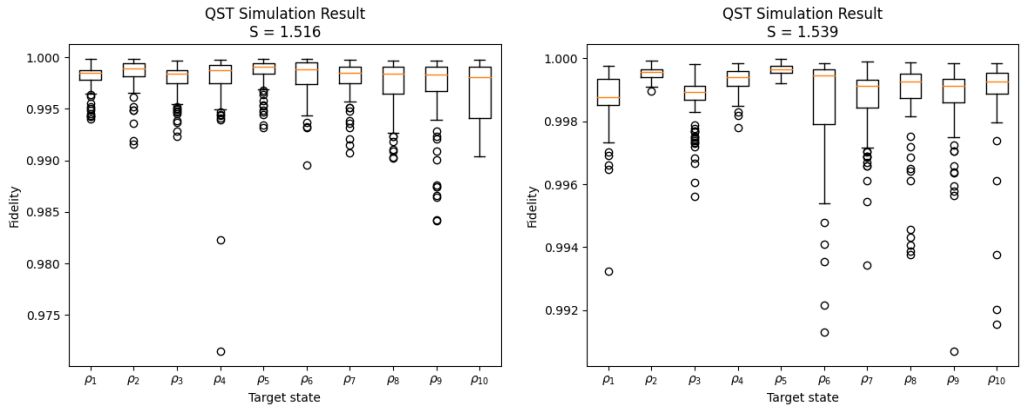

(a) PVM set with $S = 1.516$ (b) PVM set with $S = 1.539$

Figure 3.1: Monte Carlo QST Simulation Result

Figure 3.3 provides an example of the QST results obtained using the PVM sets.

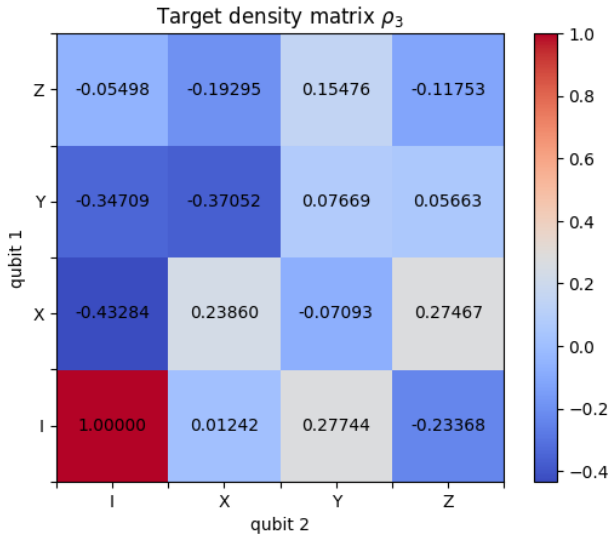

Figure 3.2: Target density matrix

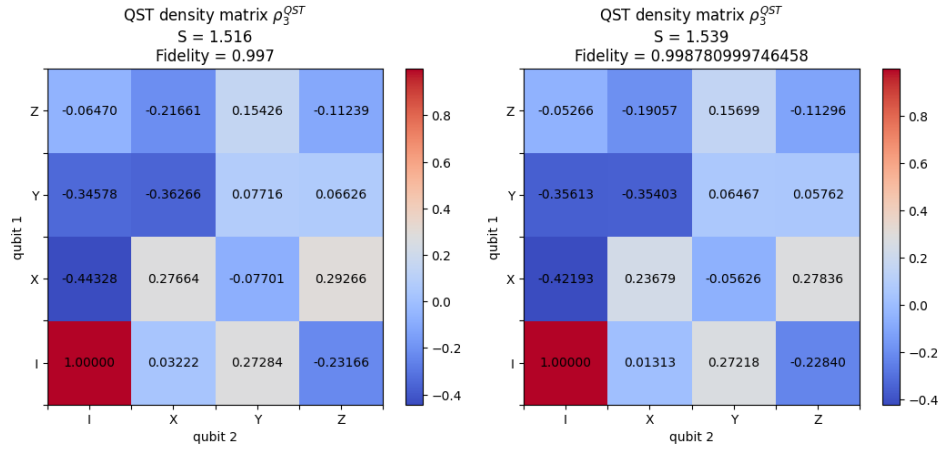

(a) QST result by the PVM set $S = 1.516$

(b) QST result by the PVM set $S = 1.539$

Figure 3.3: Monte Carlo QST Simulation Result

Chapter 4

Monte-Carlo Simulation Result

4.1 Monte-Carlo simulation process

A total of 36 prepared target states, denoted as $\{\rho^{\text{target}}ij\}_{i,j=0,1,\cdots,5}$, were employed. To ensure there is no dependence on specific target states for the given PVM operator sets, the target states were prepared to be symmetric, resulting in a symmetric gram matrix. The target states are given by:

$$\rho_{ij}^{\text{target}} = |i\rangle\langle i| \otimes |j\rangle\langle j| \tag{4.1}$$

where

$$\begin{aligned}
|0\rangle &= \begin{pmatrix} 1 \\ 0 \end{pmatrix} \\
|1\rangle &= \begin{pmatrix} 0 \\ 1 \end{pmatrix} \\
|2\rangle &= |+\rangle = \frac{1}{\sqrt{2}}(|0\rangle + |1\rangle) \\
|3\rangle &= |-\rangle = \frac{1}{\sqrt{2}}(|0\rangle - |1\rangle) \\
|4\rangle &= |i\rangle = \frac{1}{\sqrt{2}}(|0\rangle + i\,|1\rangle) \\
|5\rangle &= |-i\rangle = \frac{1}{\sqrt{2}}(|0\rangle - i\,|1\rangle)
\end{aligned}$$

4.1.1 Preparing PVM operator set

In order to investigate the entropy dependence in the QST process, PVM operator sets were constructed with various entropies. This was achieved by optimizing the value of $(S_{\text{PVM set}} - S_{\text{target entropy}})^2$ instead of directly optimizing $S_{\text{PVM set}}$. The optimization process utilized the `scipy.optimize.minimize` function. For the Monte Carlo simulation, the target entropies were set as $S_{\text{target}} = 1.350, 1.390, 1.430, 1.470, 1.510, 1.516$, where the value 1.516 served as an upper bound for using only 9 CZ gates. Twenty PVM sets were generated for each target entropy.

4.1.2 Measurement Process

In an actual experiment, a photodetector is used to count the number of photons emitted from the NV center qubit. The measurement frequency $f_i = \frac{n_i}{N}$ represents the raw data obtained from the measurement process. Here, N refers to the total number of shots, which corresponds to the total number of trials of measurement[1]. The expectation value of n_i is given by $\operatorname{Tr} \rho^{\text{target}} \Omega^i$, and the resulting error or noise in the measurement process follows a Poisson distribution. In the simulation, the values of N were set to $2500, 5625, 10000, 15625, 22500$ so that $\sqrt{N}$ was equally spaced, and the total number of shots was kept the same for all measurements. To evaluate the tolerance of the PVM operator set against Poisson error, the simulated measurement outcomes n_i were generated with Poisson error, and 100 measurements were performed for each N, PVM operator set, and target state. The `numpy.random.poisson` function was used to generate random Poisson error.

[1] See 1

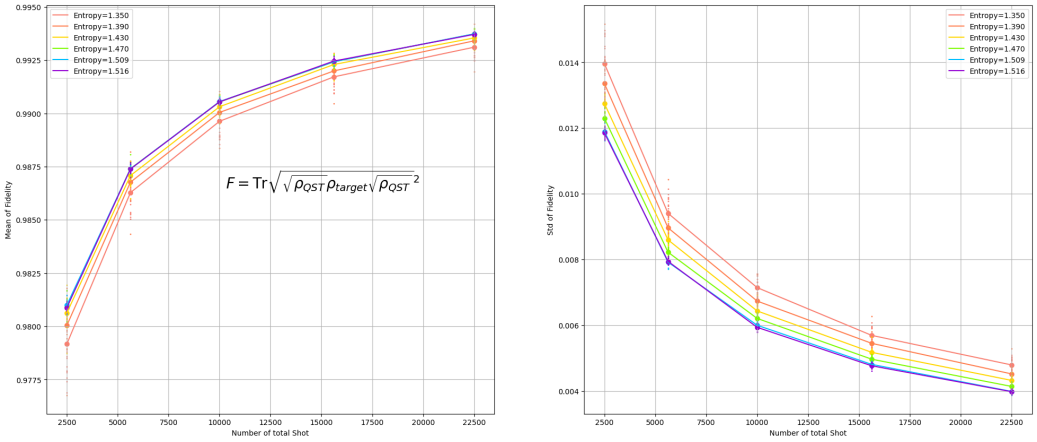

Figure 4.1: Monte Carlo simulation Result

4.2 Monte Carlo Simulation Result

4.2.1 Shot dependence

The Monte Carlo simulation results demonstrate that as Poisson noise decreases, higher fidelity is expected. Figure 4.1 displays the standard deviation for fidelity, which decreases rapidly as the number of shots increases for all target entropies. Figure 4.1 displays the mean of fidelity, which increases as the number of shots increases for all target entropies.

4.2.2 Entropy dependence

The Monte Carlo simulation results demonstrate that as Poisson noise decreases, higher fidelity is expected. Figure 4.1 displays the standard deviation for fidelity, which decreases rapidly as the number of shots increases for all target entropies. Additionally, the figure also shows the mean of fidelity, which increases as the number of shots increases for all target entropies.

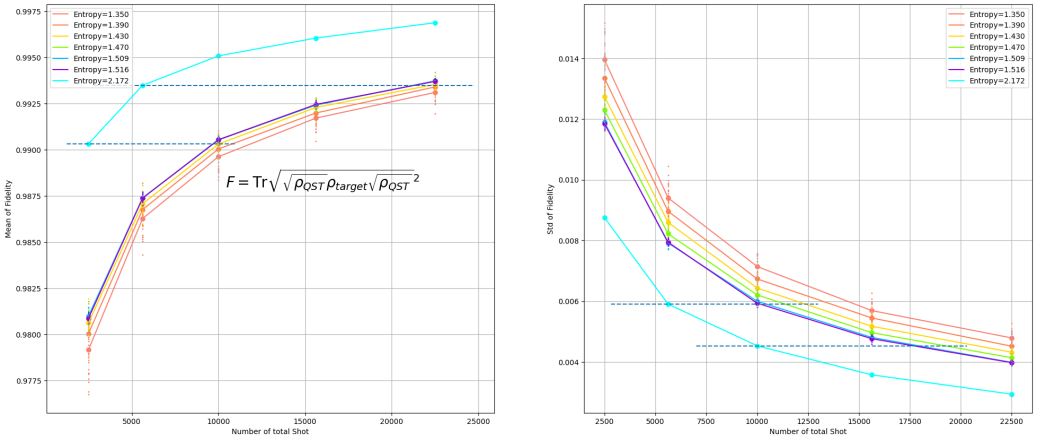

Figure 4.2: Monte Carlo simulation result for comparison

4.3 Comparison

In Section 2.4, ideal QST scenarios were introduced, including the GSIC POVM and SIC POVM. However, the SIC POVM, while the most ideal case, is hardly implementable in general setups. Therefore, a comparison is made between the PVM set generated by our strategy and the conventional PVM set.

As shown in Figure 4.2, the conventional PVM, with an entropy of 2.172, outperforms our PVM set, which has an entropy of 1.516 (the best result from our strategy) and 1.539 (GSIC POVM). However, this difference can be overcome by obtaining more photons in the measurement stage. Considering the trend that QST improves as the entropy increases, the difference between our PVM set and the GSIC POVM set is not significant.

4.3.1 Discussion: Our strategy can be better?

Clearly, our PVM set is inferior to the conventional one. To investigate why the entropy of the conventional PVM set is significantly better, let us compare the (normalized) eigenvalues of the gram matrix.

SIC POVM:

$$e_i = 0.25, 0.05, 0.05, \cdots, 0.05 \tag{4.2}$$

Convectional:

$$\begin{aligned} e_i =& 0.325, 0.143, 0.143, 0.071, 0.071, \\ & 0.063, 0.031, 0.031, 0.031, 0.031 \\ & 0.016, 0.014, 0.014, 0.007, 0.007, 0.003 \end{aligned} \tag{4.3}$$

GSIC POVM:

$$e_i = 0.667, 0.022, 0.022, \cdots, 0.022 \tag{4.4}$$

The obvious difference lies in the magnitude of the leading term. It is trivial that the largest eigenvalue corresponds to the measurement of the identity basis. However, measuring the identity basis is regarded as meaningless since it only measures the trace of the density matrix, which is trivially equal to 1 due to the normalization condition. So, can we conduct the measurement process without including measurements of the identity basis?

Unfortunately, it is impossible. The condition of positive measurement requires $\langle \Omega \rangle \geq 0$, which means Ω must include the identity measurement. In our setup, where only one detector is available, we cannot even resolve the identity component in our PVM operators. This limitation stems from the fundamental restriction of our setup. In other setups where multiple detectors are used, the identity part can be relatively resolved in the measurement operators. Therefore, in our setup, the GSIC PVM is our best option if it can be implemented successfully.

Remark 3: The Limitations of Hilbert-Schmidt Norm The Hilbert-Schmidt norm, unlike the von Neumann entropy, does not guarantee the full rank of the gram matrix or the positivity of each PVM operator. Although the diagonal gram matrix ensures the minimum Hilbert-Schmidt norm, which can be achieved with the Pauli basis, it is important to note that the Pauli basis is not positive semi-definite. Therefore, relying solely on the Hilbert-Schmidt norm may not provide a complete characterization of the measurement operators in terms of their rank and positivity.

Chapter 5

Conclusion

In Full Quantum State Tomography (FQST), a minimum of $d^2 - 1$ measurement operators is required, but to ensure the symmetric property, the PVM set consists of d^2 measurement operators. The von Neumann entropy serves as a metric to assess the stability of QST.

Our Monte Carlo simulation results have shown that higher von Neumann entropy leads to higher mean fidelity and lower standard deviation of fidelity. In our setup, the best entropy achieved was 1.539, while the optimal entropy obtained using our strategy was 1.516. In comparison, the entropy of the conventional PVM set was 2.172. However, by increasing the number of photons in the measurement stage, it is possible to overcome this difference and improve the performance of our PVM set.

Chapter 6

Appendix

6.1 Prepared density matrix

$$\rho_1 = \begin{pmatrix} 0.38 + 0.j & -0.064 - 0.044j & -0.021 + 0.062j & -0.022 - 0.034j \\ -0.064 + 0.044j & 0.202 + 0.j & -0.058 + 0.167j & 0.066 - 0.115j \\ -0.021 - 0.062j & -0.058 - 0.167j & 0.228 + 0.j & -0.092 - 0.031j \\ -0.022 + 0.034j & 0.066 + 0.115j & -0.092 + 0.031j & 0.19 + 0.j \end{pmatrix}$$

$$\rho_2 = \begin{pmatrix} 0.17 + 0.j & -0.151 - 0.024j & -0.082 + 0.097j & 0.04 + 0.053j \\ -0.151 + 0.024j & 0.466 + 0.j & 0.041 - 0.113j & 0.025 - 0.012j \\ -0.082 - 0.097j & 0.041 + 0.113j & 0.216 + 0.j & 0.003 - 0.095j \\ 0.04 - 0.053j & 0.025 + 0.012j & 0.003 + 0.095j & 0.148 + 0.j \end{pmatrix}$$

$$\rho_3 = \begin{pmatrix} 0.148 + 0.j & -0.045 - 0.108j & -0.04 + 0.073j & 0.04 + 0.11j \\ -0.045 + 0.108j & 0.324 + 0.j & 0.079 + 0.075j & -0.177 + 0.101j \\ -0.04 - 0.073j & 0.079 - 0.075j & 0.235 + 0.j & 0.051 - 0.031j \\ 0.04 - 0.11j & -0.177 - 0.101j & 0.051 + 0.031j & 0.293 + 0.j \end{pmatrix}$$

$$\rho_4 = \begin{pmatrix} 0.241 + 0.j & -0.081 + 0.101j & 0.01 - 0.036j & 0.114 - 0.108j \\ -0.081 - 0.101j & 0.192 + 0.j & -0.073 + 0.146j & -0.038 - 0.027j \\ 0.01 + 0.036j & -0.073 - 0.146j & 0.356 + 0.j & -0.049 - 0.119j \\ 0.114 + 0.108j & -0.038 + 0.027j & -0.049 + 0.119j & 0.211 + 0.j \end{pmatrix}$$

$$\rho_5 = \begin{pmatrix} 0.245 + 0.j & 0.03 + 0.068j & 0.038 + 0.068j & 0.01 - 0.j \\ 0.03 - 0.068j & 0.259 + 0.j & 0.051 + 0.009j & 0.177 - 0.117j \\ 0.038 - 0.068j & 0.051 - 0.009j & 0.143 + 0.j & 0.021 - 0.054j \\ 0.01 + 0.j & 0.177 + 0.117j & 0.021 + 0.054j & 0.353 + 0.j \end{pmatrix}$$

$$\rho_6 = \begin{pmatrix} 0.186 + 0.j & -0.023 - 0.046j & -0.01 - 0.089j & -0.062 - 0.041j \\ -0.023 + 0.046j & 0.065 + 0.j & 0.028 - 0.123j & -0.052 - 0.035j \\ -0.01 + 0.089j & 0.028 + 0.123j & 0.42 + 0.j & 0.031 - 0.16j \\ -0.062 + 0.041j & -0.052 + 0.035j & 0.031 + 0.16j & 0.33 + 0.j \end{pmatrix}$$

$$\rho_7 = \begin{pmatrix} 0.271 + 0.j & 0.078 + 0.044j & -0.059 + 0.034j & -0.079 + 0.207j \\ 0.078 - 0.044j & 0.232 + 0.j & -0.073 + 0.09j & 0.087 + 0.064j \\ -0.059 - 0.034j & -0.073 - 0.09j & 0.098 + 0.j & 0.05 + 0.015j \\ -0.079 - 0.207j & 0.087 - 0.064j & 0.05 - 0.015j & 0.4 + 0.j \end{pmatrix}$$

$$\rho_8 = \begin{pmatrix} 0.245 + 0.j & 0.048 + 0.078j & -0.014 - 0.148j & 0.112 + 0.121j \\ 0.048 - 0.078j & 0.201 + 0.j & -0.109 - 0.07j & 0.068 - 0.002j \\ -0.014 + 0.148j & -0.109 + 0.07j & 0.365 + 0.j & -0.156 + 0.166j \\ 0.112 - 0.121j & 0.068 + 0.002j & -0.156 - 0.166j & 0.189 + 0.j \end{pmatrix}$$

$$\rho_9 = \begin{pmatrix} 0.392 + 0.j & -0.183 - 0.13j & -0.246 + 0.134j & -0.019 - 0.072j \\ -0.183 + 0.13j & 0.292 + 0.j & 0.043 - 0.141j & 0.026 + 0.064j \\ -0.246 - 0.134j & 0.043 + 0.141j & 0.266 + 0.j & 0.014 + 0.036j \\ -0.019 + 0.072j & 0.026 - 0.064j & 0.014 - 0.036j & 0.049 + 0.j \end{pmatrix}$$

$$\rho_{10} = \begin{pmatrix} 0.253 + 0.j & -0.1 - 0.039j & 0.022 - 0.043j & 0.137 + 0.202j \\ -0.1 + 0.039j & 0.239 + 0.j & -0.088 + 0.039j & -0.129 - 0.083j \\ 0.022 + 0.043j & -0.088 - 0.039j & 0.192 + 0.j & 0.07 + 0.024j \\ 0.137 - 0.202j & -0.129 + 0.083j & 0.07 - 0.024j & 0.317 + 0.j \end{pmatrix}$$

6.2 PVM set $S = 1.539$

$$\Omega^1 = \begin{pmatrix} 0.456 + 0.j & 0.053 - 0.046j & 0.018 - 0.077j & 0.033 + 0.156j \\ 0.053 + 0.046j & 0.488 + 0.j & -0.114 + 0.123j & -0.01 + 0.017j \\ 0.018 + 0.077j & -0.114 - 0.123j & 0.384 + 0.j & 0.394 - 0.085j \\ 0.033 - 0.156j & -0.01 - 0.017j & 0.394 + 0.085j & 0.671 + 0.j \end{pmatrix}$$

$$\Omega^2 = \begin{pmatrix} 0.56 + 0.j & -0.034 + 0.155j & -0.249 + 0.283j & -0.138 - 0.046j \\ -0.034 - 0.155j & 0.602 + 0.j & 0.05 + 0.164j & -0.027 + 0.012j \\ -0.249 - 0.283j & 0.05 - 0.164j & 0.419 + 0.j & 0.02 - 0.132j \\ -0.138 + 0.046j & -0.027 - 0.012j & 0.02 + 0.132j & 0.419 + 0.j \end{pmatrix}$$

$$\Omega^3 = \begin{pmatrix} 0.485 + 0.j & -0.058 + 0.064j & 0.069 + 0.053j & 0.237 + 0.301j \\ -0.058 - 0.064j & 0.544 + 0.j & 0.008 + 0.037j & -0.026 - 0.111j \\ 0.069 - 0.053j & 0.008 - 0.037j & 0.392 + 0.j & -0.223 - 0.118j \\ 0.237 - 0.301j & -0.026 + 0.111j & -0.223 + 0.118j & 0.579 + 0.j \end{pmatrix}$$

$$\Omega^4 = \begin{pmatrix} 0.306 + 0.j & 0.207 - 0.084j & -0.006 + 0.179j & -0.032 - 0.104j \\ 0.207 + 0.084j & 0.377 + 0.j & 0.011 - 0.125j & 0.049 - 0.119j \\ -0.006 - 0.179j & 0.011 + 0.125j & 0.406 + 0.j & -0.053 + 0.073j \\ -0.032 + 0.104j & 0.049 + 0.119j & -0.053 - 0.073j & 0.912 + 0.j \end{pmatrix}$$

$$\Omega^5 = \begin{pmatrix} 0.408 + 0.j & 0.151 - 0.115j & 0.074 - 0.087j & -0.025 - 0.093j \\ 0.151 + 0.115j & 0.538 + 0.j & -0.112 + 0.357j & -0.074 + 0.045j \\ 0.074 + 0.087j & -0.112 - 0.357j & 0.61 + 0.j & -0.168 + 0.059j \\ -0.025 + 0.093j & -0.074 - 0.045j & -0.168 - 0.059j & 0.444 + 0.j \end{pmatrix}$$

$$\Omega^6 = \begin{pmatrix} 0.271 + 0.j & -0. + 0.104j & 0.22 - 0.049j & -0.223 + 0.047j \\ -0. - 0.104j & 0.735 + 0.j & 0.161 - 0.107j & -0.194 + 0.08j \\ 0.22 + 0.049j & 0.161 + 0.107j & 0.498 + 0.j & 0.006 - 0.035j \\ -0.223 - 0.047j & -0.194 - 0.08j & 0.006 + 0.035j & 0.495 + 0.j \end{pmatrix}$$

$$\Omega^7 = \begin{pmatrix} 0.597 + 0.j & 0.116 + 0.052j & 0.014 - 0.144j & 0.136 - 0.253j \\ 0.116 - 0.052j & 0.634 + 0.j & -0.006 - 0.1j & -0.015 - 0.197j \\ 0.014 + 0.144j & -0.006 + 0.1j & 0.436 + 0.j & 0.031 - 0.225j \\ 0.136 + 0.253j & -0.015 + 0.197j & 0.031 + 0.225j & 0.333 + 0.j \end{pmatrix}$$

$$\Omega^8 = \begin{pmatrix} 0.522 + 0.j & -0.001 - 0.039j & -0.024 + 0.11j & 0.23 - 0.089j \\ -0.001 + 0.039j & 0.539 + 0.j & -0.101 - 0.141j & -0.132 + 0.352j \\ -0.024 - 0.11j & -0.101 + 0.141j & 0.479 + 0.j & 0.004 + 0.035j \\ 0.23 + 0.089j & -0.132 - 0.352j & 0.004 - 0.035j & 0.459 + 0.j \end{pmatrix}$$

$$\Omega^{9} = \begin{pmatrix} 0.429 + 0.j & 0.09 - 0.192j & -0.115 + 0.031j & -0.093 + 0.176j \\ 0.09 + 0.192j & 0.735 + 0.j & -0.114 - 0.155j & 0.139 - 0.055j \\ -0.115 - 0.031j & -0.114 + 0.155j & 0.646 + 0.j & -0.006 + 0.054j \\ -0.093 - 0.176j & 0.139 + 0.055j & -0.006 - 0.054j & 0.19 + 0.j \end{pmatrix}$$

$$\Omega^{10} = \begin{pmatrix} 0.619 + 0.j & -0.034 - 0.177j & -0.128 - 0.095j & 0.088 + 0.005j \\ -0.034 + 0.177j & 0.525 + 0.j & 0.367 + 0.051j & -0.045 - 0.02j \\ -0.128 + 0.095j & 0.367 - 0.051j & 0.382 + 0.j & 0.041 + 0.168j \\ 0.088 - 0.005j & -0.045 + 0.02j & 0.041 - 0.168j & 0.474 + 0.j \end{pmatrix}$$

$$\Omega^{11} = \begin{pmatrix} 0.634 + 0.j & -0.155 - 0.082j & 0.165 + 0.18j & -0.002 - 0.03j \\ -0.155 + 0.082j & 0.232 + 0.j & -0.027 - 0.012j & -0.155 - 0.173j \\ 0.165 - 0.18j & -0.027 + 0.012j & 0.775 + 0.j & 0.093 + 0.047j \\ -0.002 + 0.03j & -0.155 + 0.173j & 0.093 - 0.047j & 0.359 + 0.j \end{pmatrix}$$

$$\Omega^{12} = \begin{pmatrix} 0.886 + 0.j & -0.083 - 0.03j & 0.037 - 0.091j & -0.197 + 0.005j \\ -0.083 + 0.03j & 0.438 + 0.j & -0.162 - 0.061j & -0.014 + 0.013j \\ 0.037 + 0.091j & -0.162 + 0.061j & 0.123 + 0.j & -0.1 + 0.067j \\ -0.197 - 0.005j & -0.014 - 0.013j & -0.1 - 0.067j & 0.553 + 0.j \end{pmatrix}$$

$$\Omega^{13} = \begin{pmatrix} 0.573 + 0.j & 0.052 - 0.021j & -0.074 - 0.126j & -0.093 + 0.061j \\ 0.052 + 0.021j & 0.12 + 0.j & 0.099 - 0.053j & 0.086 + 0.155j \\ -0.074 + 0.126j & 0.099 + 0.053j & 0.751 + 0.j & -0.075 - 0.236j \\ -0.093 - 0.061j & 0.086 - 0.155j & -0.075 + 0.236j & 0.555 + 0.j \end{pmatrix}$$

$$\Omega^{14} = \begin{pmatrix} 0.354 + 0.j & -0.067 + 0.248j & -0.218 - 0.181j & 0.023 + 0.009j \\ -0.067 - 0.248j & 0.418 + 0.j & -0.108 - 0.05j & -0.106 - 0.084j \\ -0.218 + 0.181j & -0.108 + 0.05j & 0.661 + 0.j & -0.006 + 0.204j \\ 0.023 - 0.009j & -0.106 + 0.084j & -0.006 - 0.204j & 0.567 + 0.j \end{pmatrix}$$

$$\Omega^{15} = \begin{pmatrix} 0.633 + 0.j & 0.112 + 0.24j & 0.182 + 0.05j & 0.049 + 0.002j \\ 0.112 - 0.24j & 0.465 + 0.j & 0.073 + 0.04j & 0.286 + 0.062j \\ 0.182 - 0.05j & 0.073 - 0.04j & 0.527 + 0.j & 0.055 + 0.17j \\ 0.049 - 0.002j & 0.286 - 0.062j & 0.055 - 0.17j & 0.375 + 0.j \end{pmatrix}$$

$$\Omega^{16} = \begin{pmatrix} 0.266 + 0.j & -0.347 - 0.077j & 0.037 - 0.036j & 0.007 - 0.144j \\ -0.347 + 0.077j & 0.609 + 0.j & -0.023 + 0.033j & 0.236 + 0.024j \\ 0.037 + 0.036j & -0.023 - 0.033j & 0.51 + 0.j & -0.014 - 0.044j \\ 0.007 + 0.144j & 0.236 - 0.024j & -0.014 + 0.044j & 0.615 + 0.j \end{pmatrix}$$

6.3 PVM set $S = 1.516$

$$\Omega^1 = \begin{pmatrix} 0.468 + 0.j & -0.103 + 0.149j & 0.143 - 0.017j & 0. + 0.j \\ -0.103 - 0.149j & 0.123 + 0.j & 0. + 0.j & 0.143 - 0.017j \\ 0.143 + 0.017j & 0. - 0.j & 0.877 + 0.j & -0.103 + 0.149j \\ 0. + 0.j & 0.143 + 0.017j & -0.103 - 0.149j & 0.532 + 0.j \end{pmatrix}$$

$$\Omega^2 = \begin{pmatrix} 0.727 + 0.j & -0.216 - 0.112j & 0.004 + 0.186j & 0. - 0.j \\ -0.216 + 0.112j & 0.608 + 0.j & 0. + 0.j & 0.004 + 0.186j \\ 0.004 - 0.186j & 0. - 0.j & 0.392 + 0.j & -0.216 - 0.112j \\ 0. + 0.j & 0.004 - 0.186j & -0.216 + 0.112j & 0.273 + 0.j \end{pmatrix}$$

$$\Omega^3 = \begin{pmatrix} 0.617 + 0.j & 0.077 - 0.227j & 0.097 - 0.226j & -0. - 0.j \\ 0.077 + 0.227j & 0.473 + 0.j & 0. + 0.j & 0.097 - 0.226j \\ 0.097 + 0.226j & 0. + 0.j & 0.527 + 0.j & 0.077 - 0.227j \\ -0. + 0.j & 0.097 + 0.226j & 0.077 + 0.227j & 0.383 + 0.j \end{pmatrix}$$

$$\Omega^4 = \begin{pmatrix} 0.596 + 0.j & -0.035 + 0.228j & -0.036 - 0.156j & -0. + 0.j \\ -0.035 - 0.228j & 0.788 + 0.j & -0. + 0.j & -0.036 - 0.156j \\ -0.036 + 0.156j & -0. - 0.j & 0.212 + 0.j & -0.035 + 0.228j \\ -0. + 0.j & -0.036 + 0.156j & -0.035 - 0.228j & 0.404 + 0.j \end{pmatrix}$$

$$\Omega^5 = \begin{pmatrix} 0.094 + 0.j & -0.101 - 0.082j & -0.156 - 0.034j & 0. + 0.j \\ -0.101 + 0.082j & 0.521 + 0.j & 0. - 0.j & -0.156 - 0.034j \\ -0.156 + 0.034j & 0. + 0.j & 0.479 + 0.j & -0.101 - 0.082j \\ 0. + 0.j & -0.156 + 0.034j & -0.101 + 0.082j & 0.906 + 0.j \end{pmatrix}$$

$$\Omega^6 = \begin{pmatrix} 0.34 + 0.j & 0.192 + 0.017j & 0.184 + 0.169j & -0. + 0.j \\ 0.192 - 0.017j & 0.659 + 0.j & -0. + 0.j & 0.184 + 0.169j \\ 0.184 - 0.169j & -0. - 0.j & 0.341 + 0.j & 0.192 + 0.017j \\ -0. + 0.j & 0.184 - 0.169j & 0.192 - 0.017j & 0.66 + 0.j \end{pmatrix}$$

$$\Omega^7 = \begin{pmatrix} 0.66 + 0.j & 0.186 + 0.028j & -0.237 + 0.078j & 0. + 0.j \\ 0.186 - 0.028j & 0.33 + 0.j & -0. + 0.j & -0.237 + 0.078j \\ -0.237 - 0.078j & -0. - 0.j & 0.67 + 0.j & 0.186 + 0.028j \\ 0. + 0.j & -0.237 - 0.078j & 0.186 - 0.028j & 0.34 + 0.j \end{pmatrix}$$

$$\Omega^8 = \begin{pmatrix} 0.563 + 0.j & 0.079 - 0.198j & 0.222 + 0.059j & -0.068 + 0.027j \\ 0.079 + 0.198j & 0.437 + 0.j & 0.191 - 0.063j & -0.221 - 0.059j \\ 0.222 - 0.059j & 0.191 + 0.063j & 0.437 + 0.j & -0.08 + 0.198j \\ -0.068 - 0.027j & -0.221 + 0.059j & -0.08 - 0.198j & 0.563 + 0.j \end{pmatrix}$$

$$\Omega^{9} = \begin{pmatrix} 0.531 + 0.j & 0.129 + 0.211j & 0.117 - 0.218j & -0.033 - 0.026j \\ 0.129 - 0.211j & 0.468 + 0.j & 0.017 + 0.027j & -0.117 + 0.218j \\ 0.117 + 0.218j & 0.017 - 0.027j & 0.468 + 0.j & -0.129 - 0.211j \\ -0.033 + 0.026j & -0.117 - 0.218j & -0.129 + 0.211j & 0.533 + 0.j \end{pmatrix}$$

$$\Omega^{10} = \begin{pmatrix} 0.359 + 0.j & -0.127 + 0.13j & 0.015 + 0.143j & -0.145 - 0.038j \\ -0.127 - 0.13j & 0.641 + 0.j & 0.206 + 0.195j & -0.015 - 0.142j \\ 0.015 - 0.143j & 0.206 - 0.195j & 0.641 + 0.j & 0.127 - 0.131j \\ -0.145 + 0.038j & -0.015 + 0.142j & 0.127 + 0.131j & 0.359 + 0.j \end{pmatrix}$$

$$\Omega^{11} = \begin{pmatrix} 0.642 + 0.j & -0.104 + 0.1j & 0.102 + 0.151j & 0.123 + 0.087j \\ -0.104 - 0.1j & 0.358 + 0.j & -0.274 - 0.059j & -0.102 - 0.151j \\ 0.102 - 0.151j & -0.274 + 0.059j & 0.359 + 0.j & 0.104 - 0.1j \\ 0.123 - 0.087j & -0.102 + 0.151j & 0.104 + 0.1j & 0.641 + 0.j \end{pmatrix}$$

$$\Omega^{12} = \begin{pmatrix} 0.63 + 0.j & 0.134 + 0.005j & -0.204 + 0.055j & 0.106 + 0.209j \\ 0.134 - 0.005j & 0.37 + 0.j & 0.143 + 0.123j & 0.204 - 0.055j \\ -0.204 - 0.055j & 0.143 - 0.123j & 0.37 + 0.j & -0.134 - 0.005j \\ 0.106 - 0.209j & 0.204 + 0.055j & -0.134 + 0.005j & 0.63 + 0.j \end{pmatrix}$$

$$\Omega^{13} = \begin{pmatrix} 0.616 + 0.j & -0.208 - 0.038j & -0.114 - 0.132j & -0.124 - 0.055j \\ -0.208 + 0.038j & 0.383 + 0.j & 0.101 - 0.211j & 0.114 + 0.131j \\ -0.114 + 0.132j & 0.101 + 0.211j & 0.384 + 0.j & 0.208 + 0.038j \\ -0.124 + 0.055j & 0.114 - 0.131j & 0.208 - 0.038j & 0.617 + 0.j \end{pmatrix}$$

$$\Omega^{14} = \begin{pmatrix} 0.441 + 0.j & -0.057 - 0.162j & -0.008 - 0.123j & -0.042 + 0.056j \\ -0.057 + 0.162j & 0.559 + 0.j & -0.233 + 0.308j & 0.008 + 0.123j \\ -0.008 + 0.123j & -0.233 - 0.308j & 0.559 + 0.j & 0.057 + 0.161j \\ -0.042 - 0.056j & 0.008 - 0.123j & 0.057 - 0.161j & 0.441 + 0.j \end{pmatrix}$$

$$\Omega^{15} = \begin{pmatrix} 0.253 + 0.j & 0.012 - 0.014j & -0.021 - 0.026j & 0.165 + 0.19j \\ 0.012 + 0.014j & 0.747 + 0.j & -0.02 - 0.247j & 0.022 + 0.026j \\ -0.021 + 0.026j & -0.02 + 0.247j & 0.748 + 0.j & -0.012 + 0.014j \\ 0.165 - 0.19j & 0.022 - 0.026j & -0.012 - 0.014j & 0.252 + 0.j \end{pmatrix}$$

$$\Omega^{16} = \begin{pmatrix} 0.477 + 0.j & 0.061 - 0.039j & -0.06 + 0.04j & 0.218 - 0.424j \\ 0.061 + 0.039j & 0.523 + 0.j & -0.023 + 0.001j & 0.06 - 0.04j \\ -0.06 - 0.04j & -0.023 - 0.001j & 0.523 + 0.j & -0.061 + 0.037j \\ 0.218 + 0.424j & 0.06 + 0.04j & -0.061 - 0.037j & 0.477 + 0.j \end{pmatrix}$$

Bibliography

[1] Zhibo Hou, Han-Sen Zhong, Ye Tian, Daoyi Dong, Bo Qi, Li Li, Yuanlong Wang, Franco Nori, Guo-Yong Xiang, Chuan-Feng Li, et al. Full reconstruction of a 14-qubit state within four hours. *New Journal of Physics*, 18(8):083036, 2016.

[2] Daniel FV James, Paul G Kwiat, William J Munro, and Andrew G White. Measurement of qubits. *Physical Review A*, 64(5):052312, 2001.

[3] Jae Kwang Kim and Jun Shao. *Statistical methods for handling incomplete data*. CRC press, 2021.

[4] Joseph M Renes, Robin Blume-Kohout, Andrew J Scott, and Carlton M Caves. Symmetric informationally complete quantum measurements. *Journal of Mathematical Physics*, 45(6):2171–2180, 2004.

[5] John A Smolin, Jay M Gambetta, and Graeme Smith. Efficient method for computing the maximum-likelihood quantum state from measurements with additive gaussian noise. *Physical review letters*, 108(7):070502, 2012.

[6] Yong Siah Teo, Huangjun Zhu, Berthold-Georg Englert, Jaroslav Řeháček, and Zdeněk Hradil. Quantum-state reconstruction by maximizing likelihood and entropy. *Physical review letters*, 107(2):020404, 2011.

[7] Masakazu Yoshida and Gen Kimura. Construction of general symmetric-informationally-complete–positive-operator-valued measures by using a complete orthogonal basis. *Physical Review A*, 106(2):022408, 2022.